OUT-OF-PLANE MOTION MICROACTUATORS MADE OF THIN FILM METALLIC GLASS

Seiichi Hata
Precision and Intelligence Laboratory, Tokyo Institute of Technology (Tokyo Tech.), R2-37, 4259 Nagatsuta, Midori-ku, Yokohama, 226-8503, Japan.
shata@pi.titech.ac.jp

Takashi Fukushige
Precision and Intelligence Laboratory, Tokyo Tech., R2-37, 4259 Nagatsuta, Midori-ku, Yokohama, 226-8503, Japan.
takafukushige@pi.titech.ac.jp

Takehiko Hayashi
Department of Mechano-Micro Engineering, Tokyo Tech., R2-37, 4259 Nagatsuta, Midori-ku, Yokohama, 226-8503, Japan.
t884@nano.pi.titech.ac.jp

Hiroyuki Tachikawa
Precision and Intelligence Laboratory, Tokyo Tech., R2-37, 4259 Nagatsuta, Midori-ku, Yokohama, 226-8503, Japan.
tachi@pi.titech.ac.jp

Akira Shimokohbe
Precision and Intelligence Laboratory, Tokyo Tech., R2-37, 4259 Nagatsuta, Midori-ku, Yokohama, 226-8503, Japan.
shimo@pi.titech.ac.jp

Abstract. *Two types of new out-of-plane motion electrostatic microactuators made of thin film metallic glass (TFMG) are described. TFMG is a kind of amorphous alloy thin film. It has elastic properties superior to conventional metals at room temperature. Upon heating to a specific temperature range, the supercooled liquid region, TFMG softens and can be deformed into a three-dimensional structure. In the first electrostatic microactuator named the 'conical spring linear actuator' that has 200 micrometers stroke in an out-of-plane direction. The conical-spring-shape moving electrode is made of Pd based TFMG. We introduce two variations of CSLAs. One is a multi-step motion CSLA that demonstrates nine-step motion vertical to the substrate. The other is an integrated CSLA that has one hundred actuators with a 1-mm interval on a substrate. A second microactuator, the 'out-of-plane analog motion microactuator', is also demonstrated. This actuator is a curled-up type electrostatic microactuator, which designs full-range stabilization with prevention of pull-in effect. The actuator incorporates a curled moving electrode and a taper-shaped substrate electrode. A prototype is fabricated and its driving characteristics are examined. The prototype has a 2,000-micrometer long, 250-micrometer wide and 5-micrometer thick curled-up moving electrode. In order to curl the cantilever, a bi-layered metal with a Pd based TFMG layer and a Cr layer is employed. The stable motion range is extended to 77% by a square-wave AC voltage having a 1-kHz frequency.*

Keywords*: MEMS, microactuator, electrostatic, three-dimensional, thin film metallic glass*

1. Introduction

Out-of-plane motion microactuators can be used for new MEMS devices, such as variable micro-inductors, micro-optical systems, tactile displays, active braille devices and active probes. In recent years, Hata *et al.*, (1999) have been studying a new MEMS material called thin film metallic glass (TFMG). TFMG is an amorphous, homogeneous and isotropic material. Hence, it is free from defects resulting from crystalline structures. TFMG softens and shows viscous flow in a certain temperature range, called the supercooled liquid region (SCLR), which allows for three-dimensional microforming (Hata *et al.*, 2005). Three-dimensional microformed TFMG can be employed for moving parts in out-of-plane motion microactuators through the use of its own high elastic limit. Using the properties of TFMG, we have developed several new microactuators having three-dimensional structures that allow for out-of-plane motion, such as an electrostatically-driven micro-lens actuator for high capacity magneto-optical disk drives (Hata *et al.*, 2002) and a two-degrees-of-freedom microactuator actuated by PZT films (Hata *et al.*, 2004).

This paper introduces two types of electrostatic microactuators made of a Pd-based TFMG. The first is named the conical spring linear actuator (CSLA). A conical spring-shaped moving electrode distinguishes the CSLA from conventional electrostatic microactuators. Owing to the moving electrode, the CSLA is capable of a large stroke motion vertical to the substrate. The second type of microactuator is an out-of-plane analog motion microactuator. This actuator is a curled-up type electrostatic microactuator, which has full-range stabilization with prevention of pull-in effect. The actuator consists of a curled moving electrode that delivers a large deflection in an out-of-plane direction and a taper-shaped substrate electrode.

2. Thin film metallic glass and its fabrication process

Figure 1 shows the characteristics of metallic glass. Metallic glass is a type of amorphous alloy and is an isotropic and homogenous material. With the advent of metallic glass, which has a low critical cooling rate, a high thermal stability with respect to crystallization and wide SCLR range, there has been great interest in developing this promising material over the last decade (Inoue, 2000). In order to use metallic glass for MEMS applications, the present authors have previously successfully fabricated thin film metallic glass (TFMG) using a RF-magnetron sputtering method, and have reported its thermal, mechanical and electrical properties (Liu *et al.*, 2001). TFMG is also an amorphous, isotropic and homogenous thin film material. Designs for use in MEMS made of TFMG are simplified because size effects are small and anisotropy need not be considered because of the isotropic properties and homogeneity of TFMG. In this paper, Pd-based ($Pd_{76}Cu_7Si_{17}$, atomic%) TFMG had been used. Table 1 shows the properties of the Pd-based TFMG compared with those of polysilicon and stainless steel. The TFMG exhibits an elastic limit higher than that of polysilicon and stainless steel.

The lift-off method is mainly used for patterning of Pd-based TFMG. The selection of the lift-off method originates in the high corrosion resistance of the TFMG, and the large film thickness of the structure peculiar to MEMS. Moreover, the TFMG softens in the SCLR temperature range, which enables it to be easily formed into three-dimensional shapes. The viscous flow of the TFMG in the SCLR is useful for annealing and relaxing residual and/or elastic stresses in the TFMG structures, which improves the form stability.

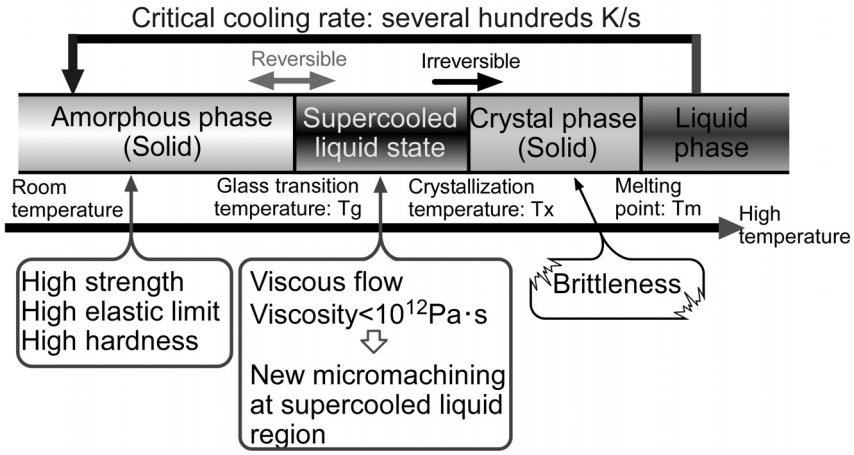

Figure 1. Characteristics of metallic glass

Table 1. Properties of the Pd-based TFMG compared with those of polysilicon and stainless steel

	Pd based TFMG ($Pd_{76}Cu_7Si_{17}$)	Polysilicon (Sharpe *et al.* 2001)	Stainless steel (SUS304)
Tg, Tx, ΔTx	637 K, 669 K, 32 K		
Young's modulus E	57.9 GPa by tensile test 69.7 GPa by bending test	170 GPa	197 GPa
Tensile strength σ	1.14 GPa	1.21 GPa	0.5 GPa
σ / E	0.020	0.007	0.003
Elastic limit	1.97 %	0.71 %	Less than 0.2 %
Hardness	Hv 515.0	N.A.	Hv 540
Reflectance	0.7 (λ=1,500 nm)	0.3 (λ=1,500 nm)	N.A.
Density	10.42×10^3 kg/m^3	10.42×10^3 kg/m^3	10.42×10^3 kg/m^3

3. Conical spring linear actuator (CSLA)

We have developed two variations of the CSLA. The first is a multi-step motion CSLA which is capable of multi-step motion vertical to the substrate. The other is an integrated CSLA which has high integration (scale: 100 actuators, density: 1 mm^2/actuator). Figure 2 shows the fundamental structure of a CSLA. The moving electrode, shaped as a conical spring is attracted to the substrate electrode by electrostatic force.

The conical spring shape can be realized by using the Pd-based TFMG and can be formed from a planar spiral spring into a three-dimensional conical spring in the SCLR. To form integrated conical springs simultaneously, we utilized photosensitive polyimide as an adhesion layer and photolithography. Figure 3 shows the schematic of the forming process of the conical spring. Initially, the substrate electrode, wiring layer and the insulating layer are fabricated. The substrate electrode and wiring are made of Ti and the insulator is made from SiO_2. Next, planar spiral beams of the Pd-based TFMG are fabricated via sputtering, lift-off patterning and sacrificial layer etching, as shown in Fig. 3(a).

As shown in Fig. 3(b) ~ 3(e), photosensitive polyimide is then spin-coated on the chip, to which a glass plate is then adhered. Subsequently, the chip, polyimide and glass plate are baked at 80ºC in order to harden the polyimide. The polyimide is patterned to remove the non-bonded part by exposure to ultraviolet light via photolithography, and the bonded part of the polyimide is then developed.

In Fig. 3(f), the glass plate is lifted vertically by 200 μm in order to deform the planar beam into a conical spring. The conical spring assembly is heated to the SCLR (637 K ~ 669 K) in a vacuum of 10^{-4} Pa by infrared heating and the elastic stress is then relaxed by the softening of the TFMG in the SCLR (Fig. 3(g)). Next, the shapes of the conical springs are fixed by cooling. Finally, polyimide is dissolved by tetra-methyl-ammonium hydroxide in order to detach the glass plate (Fig. 3(h)).

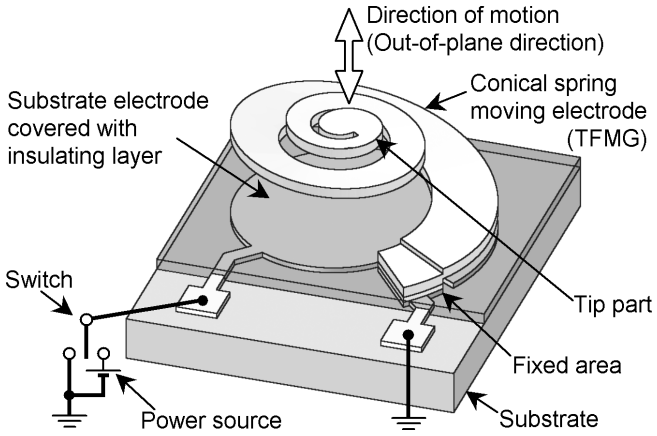

Figure 2. Fundamental structure of a CSLA

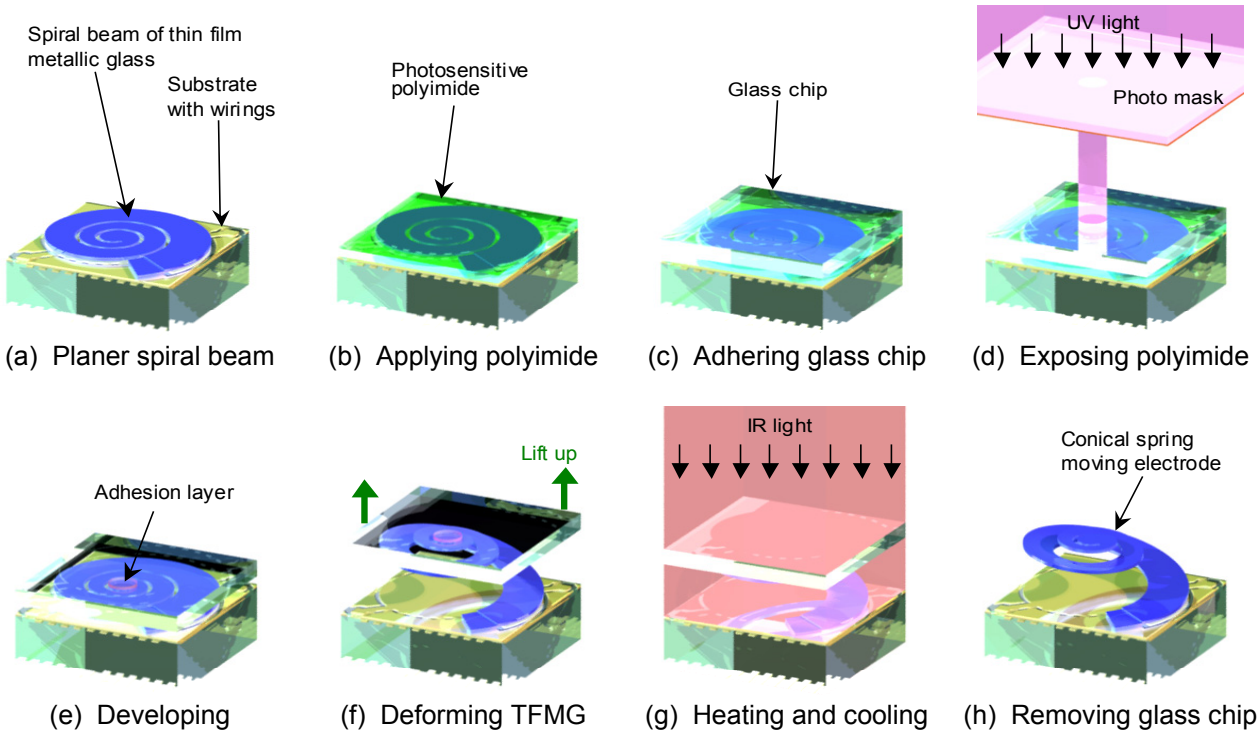

Figure 3. Three-dimensional micro-forming process for a conical spring

3.1. Multi-step motion CSLA

The multi-step motion CSLA has four distinct substrate electrodes. The two key features of the CSLA are the long vertical stroke distance with respect to the substrate surface plane and a greater number of steps than the number of substrate electrodes. Figure 4 shows a photograph of the fabricated multi-step CSLA. Four CSLAs of 600 μm basal diameter and 200 μm height were integrated on a SiO_2 substrate at 2 mm intervals. Figure 5 shows the experimental results of the displacement characteristics of the CSLA when a constant voltage is applied sequentially to the substrate electrodes and the moving electrode. In Figure 5, the sequential nine states of the four-electrode activation resulted in 200 μm stepwise displacement of the moving electrode. However, the height of this actuator did not change in steps 17 and 18. This may be due to sticking of the moving electrode to the substrate electrode.

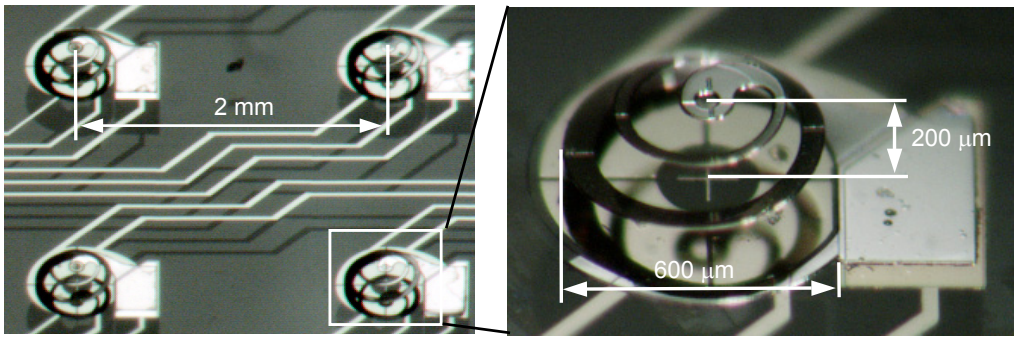

Figure 4. Fabricated multi-step motion CSLA

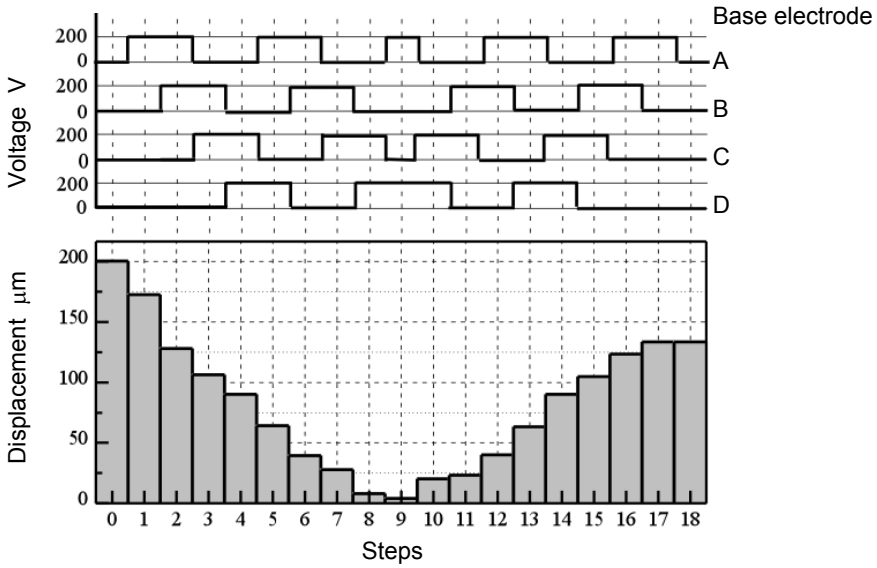

Figure 5. Displacement of the moving electrode of the multi-step motion CSLA

3.2. Integrated CSLA

In comparison with the multi-step motion CSLA, the integrated CSLA is improved in a number of aspects such as maximum output force, integration scale and integration density. In order to make the maximum output force higher, we improved the shape of the conical spring moving electrode. The maximum output force is defined as the restoring force for conical spring pushed completely to the substrate. A comparison of the moving electrode shape of the multi-step motion CSLA and the integrated CSLA is shown in Fig. 6. As a result, the maximum output force of the integrated CSLA increases up to 0.83 mN (9.5 times that of the multi-step motion CSLA). Moreover, we changed the size of the substrate to a larger one to increase the scale of integration and to utilize multilayer interconnections in order to increase the density of the integration. The SiO_2 substrate area changed from 255 mm^2 to 400 mm^2, and the scale of integration increased from 4 actuators up to 100 actuators. Figure 7 shows the structure of the integrated CSLA and the fabricated one.

A 170V square-wave AC voltage was applied to each column of the integrated CSLA sequentially using alternating-field depolarization (Fukushige *et al.*, 2005). However about 16 actuators broke during fabrication and a drive (Video is available at Shimokohbe (2005)). When one actuator was driven, there was no influence on any nearby actuators.

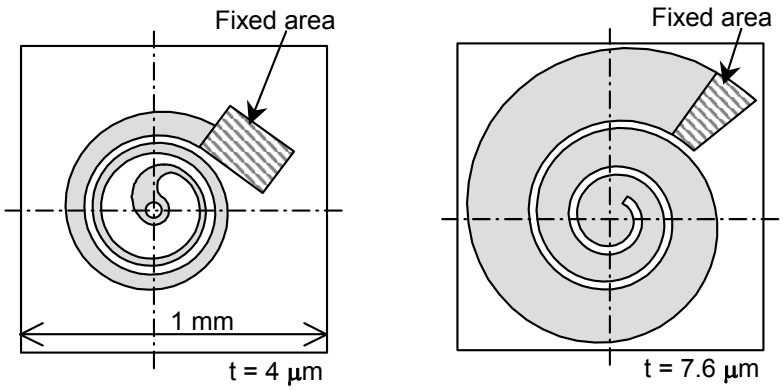

Figure 6. Comparison of the moving electrode shape of the multi-step motion CSLA and the integrated CSLA

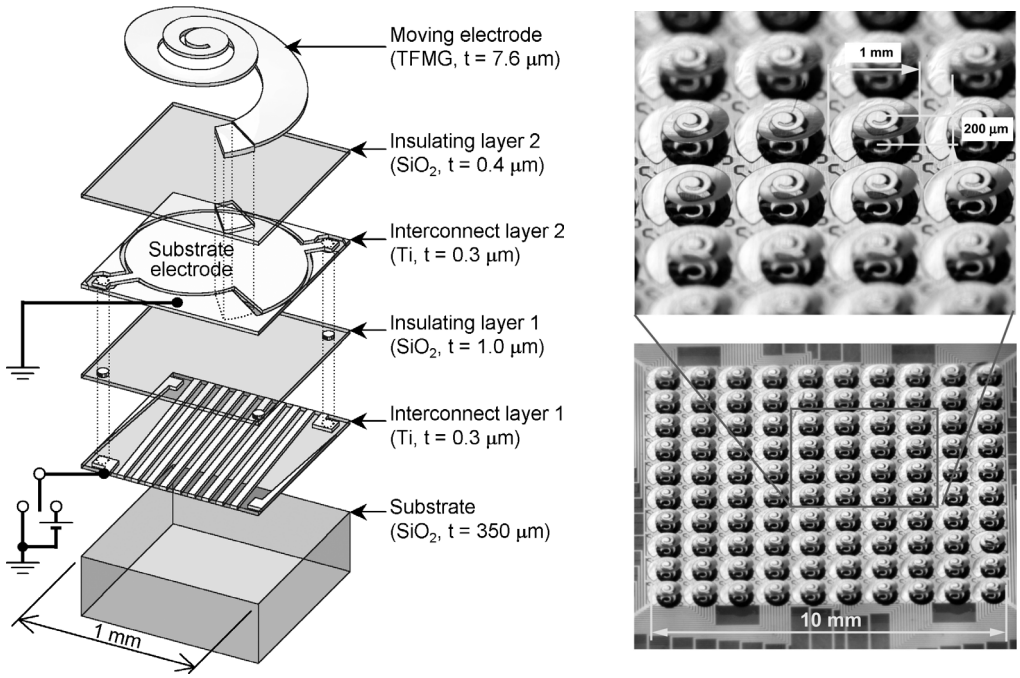

Figure 7. Structure of the integrated CSLA and fabricated one

4. Out-of-plane analog motion microactuator

A curled-up cantilever driven by an electrostatic force can especially move over large distances in an out-of-plane direction. The above-mentioned moving electrode of CSLAs is considered to be one kind of a curled-up cantilever. It is, however, difficult to achieve stability of a system that uses a cantilever (curled-up moving electrode) over the full motion range because of the pull-in effect. The realization of full-range stabilization while preventing the pull-in effect will greatly extend the applications of curled-up type electrostatic microactuators. M. Elwenspoek, *et al.* (1992) have achieved the extension of the stable motion range using a taper-shaped substrate electrode. M. A Rosa, *et al.* (2004) have also achieved full-range stable motion by placing tapered substrate electrodes on both sides of a curled-up moving electrode. We herein present the design and driving methodology of an out-of-plane analog motion microactuator using a curled-up moving electrode to extend the stable motion range without the use of a closed loop control system.

4.1 Modeling

A curled-up moving electrode achieves full-range stable analog motion on the stipulation that there is one equilibrium position at which the electrostatic force and the elastic force of the moving electrode become equal. As a methodology for realizing this stipulation, we adopt the method of using a taper-shaped substrate electrode for changing the distribution of electrostatic force (M. Elwenspoek, *et al.* (1992)). The electrostatic force *Fe (h, V)* and the elastic force *Fr (h)* are derived from the width of a substrate electrode *w(x)* as a function of the direction *x*. Figure 8 shows the structure and the deflection model of an out-of-plane analog motion microactuator employed in the present study.

It is inherently difficult to derive an accurate deflection curve for a cantilever in an electrostatic microactuator since the differential equation of deformation and electrostatic force is nonlinear. Therefore, we assume that the deflection can be expressed by simple equation. The deflection curve in the absence of an applied voltage can be expressed by equation (1).

$$y = \frac{\phi}{2} x^2 \tag{1}$$

Here, ϕ is the curvature of the cantilever and x is the lateral distance from the anchor. As shown in Fig. 8(b), the moving electrode is deflected as the contact area with the insulator increases with increasing applied voltage. The deflection curve with applied voltage is supposed to be expressed by equation (2).

$$y = d(x) = \begin{cases} 0 & (0 \le x \le x_s) \\ \frac{\phi}{2}(x - x_s)^2 & (x_s < x \le L) \end{cases} \tag{2}$$

Here, x_s is the length of the contact area and L is the length of the cantilever. It is also assumed that the curvature ϕ is constant and independent of the applied voltage and the position. It is assumed that the tip displacement of the moving electrode h is given by equation (3) as a function of the length x_s.

$$h = d(L) = \frac{\phi}{2}(L - x_s)^2 \tag{3}$$

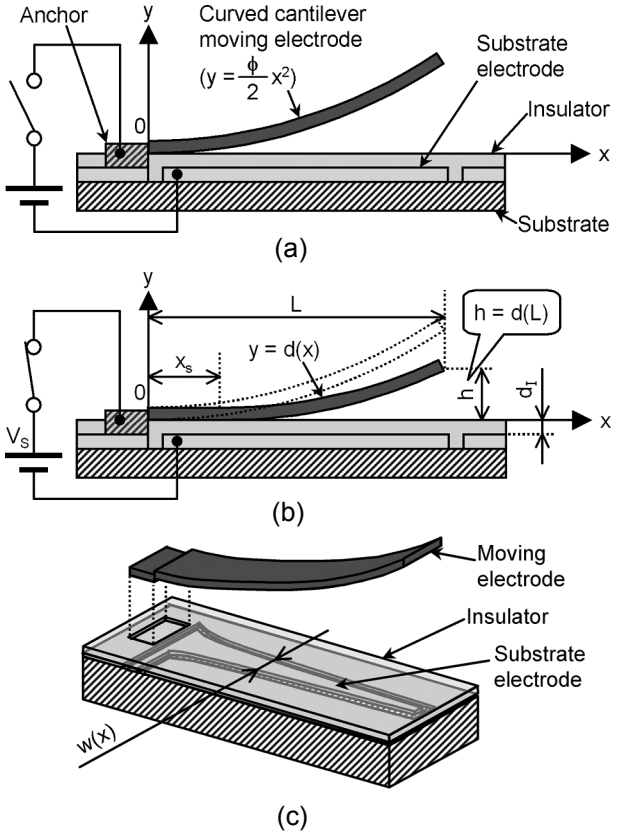

Figure 8. Structure and the deflection model

The electrostatic force *Fe (h, V)* and the elastic force *Fr (h)*, which were derived based on the above-mentioned assumptions, are shown in equations (4) and (5).

$$F_e(h,V) = \frac{1}{2} V^2 \sqrt{\frac{\phi}{2h}} \int_{L-\sqrt{\frac{2h}{\phi}}}^{L} \frac{\varepsilon w_{(x)}}{\left\{ d_i / \varepsilon_r + \frac{\phi}{2}\left(x - L + \sqrt{\frac{2h}{\phi}} \right)^2 \right\}^2} dx \tag{4}$$

$$F_r(h) = -\frac{\partial U_r}{\partial h} = EI\sqrt{\frac{\phi^3}{8h}} \tag{5}$$

We can solve *Fe (h, V) = Fr (h)* to obtain the value of h at each applied voltage V. The estimation of voltage-to-displacement characteristics thus becomes possible using the width of a substrate electrode *w(x)*.

4.2 Design and fabrication

In order to curl the cantilever in the out-of-plane direction, a bi-layered metal consisting of a 4.5-μm thick Pd based TFMG layer and a 0.5-μm thick Cr layer is employed. The difference in the internal stress in each layer at the time of deposition of the cantilever is high. Therefore, it curls automatically after deposition. The bending of the moving electrode was measured and an approximation curve was determined as equation (6).

$$y = (1.35 \times 10^{-4}) x^2 \tag{6}$$

The substrate electrode chose function *w(x)* like equation (7) so that the voltage-to-displacement characteristic becomes closer to a linear function. Figure 9 shows a calculated voltage-to-displacement characteristics and a fabricated microactuator with dimensions based on this design.

$$w(x) = \frac{3.91\times10^4}{x+1.98\times10^2} + 2.2 \tag{7}$$

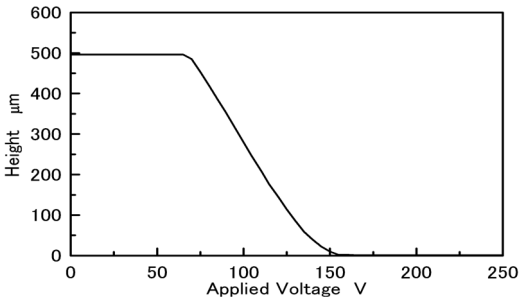

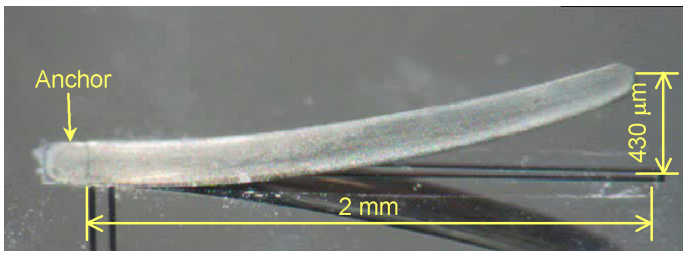

Figure 9. Calculated voltage-to-displacement characteristic and fabricated microactuator.

4.3 Driving characteristics

In order to prevent the substrate from charging, AC voltage is employed rather than DC voltage. (Fukushige *et al.*, 2005). Figure 10 shows the measured voltage-to-displacement characteristics using AC voltage. The applied voltage is a square-wave with a 1-kHz or 2-kHz frequency and an amplitude of 0 to 400 V. The stable motion range is extended to 77% when the actuator is driven by an AC voltage. Furthermore, there is no unstable behavior using AC voltage for driving the actuator.

The applied voltage for 77% displacement is 400 V, which is higher than the calculated value due to the presence of particles on the surface of the insulating layer. These particles increase the gap between the electrodes when the moving electrode contacts the insulating layer. A new model, which incorporates the existence of the particles, is expressed by equation (8).

$$y = d(x) = \begin{cases} d_P & (0 \le x \le x_S) \\ \dfrac{\phi}{2}(x - x_S)^2 + d_P & (x_S < x \le L) \end{cases} \tag{8}$$

Here, *dp* is gap resulting from the particles. The recalculated driving characteristics using this model for several values of d_P are also shown in Fig. 10. These characteristics coincide more with the actual behavior than the calculations without particles.

In Fig.10, driving of the actuator by the applied voltage of 1 kHz AC is lower than for 2 kHz. This is likely due to the influence of the switching time of the square-wave applied voltage, namely, the reduction in electrostatic force at applied voltage near zero. However, the vibration of the tip of the moving electrode caused by 1 kHz AC voltage is higher than for 2 kHz because the applied voltage frequency of 1 kHz is closer to the eigen frequency of the cantilever (600 Hz). Figure 11 shows the vibrations measured using a laser Doppler vibrometer.

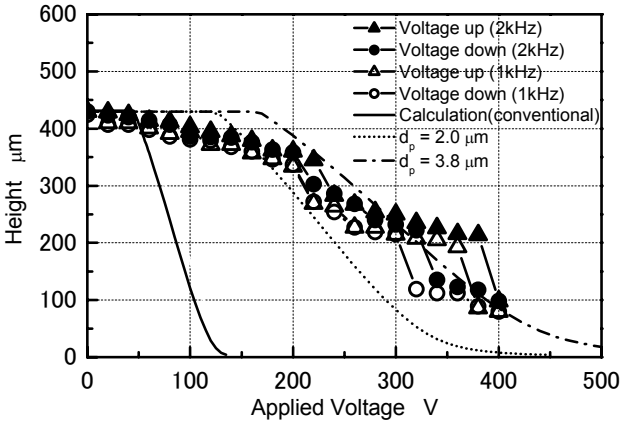

Figure 10. AC driving characteristics

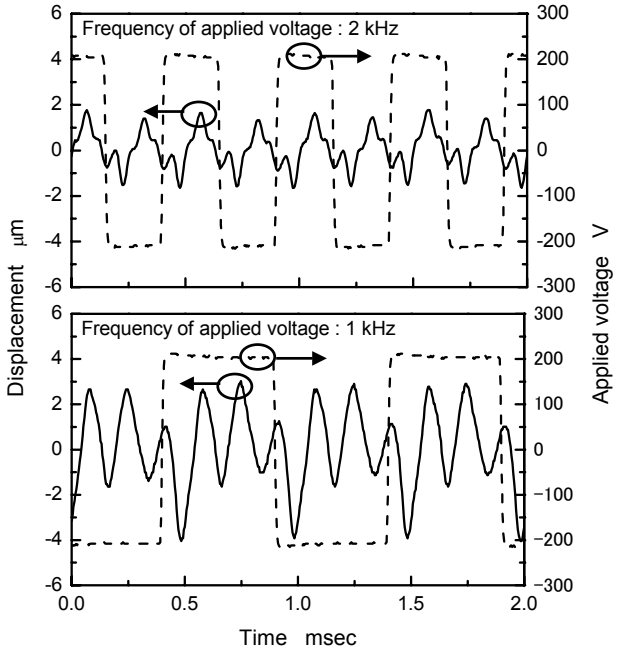

Figure 11. Vibration caused by AC driving applied voltage

5. Conclusion

In the present paper, the authors discuss two different types of electrostatic out-of-plane motion microactuators made of Pd-based TFMG, and their characteristics. The TFMG has elastic properties superior to conventional metals at room temperature. On heating the TFMG above the SCLR, it softens and can be deformed into a three-dimensional structure.

One electrostatic microactuator, named the 'CSLA: conical-spring linear actuator', could be actuated for about 200 μm, in an out-of-plane direction. The conical-spring-shaped moving electrode was made of TFMG. We introduced two variations of CSLAs. One was a multi-step motion CSLA which demonstrated nine-step motion vertical to the substrate. The other was an integrated CSLA which had a 200 μm stroke in the out-of-plane direction, maximum 0.83mN output force and high integration (scale: 100 actuators, density: 1 mm^2/actuator).

A second microactuator, the 'out-of-plane analog motion microactuator', was also demonstrated. This actuator consisted of a curled moving electrode that delivers a large deflection in an out-of-plane direction and a taper-shaped substrate electrode. A prototype was fabricated and its driving characteristics were examined. The stable motion range was extended to 77% by using a square-wave AC voltage. Further work is currently in progress to study feedback control of the microactuators with sensor-less control or by using a built-in sensor.

6. Acknowledgements

This research was supported by a grant from the Japan Society for the Promotion of Science (JSPS), Grant-in-aid for Scientific Research (A), 15206015, 2005. The authors also express their gratitude to the MEMS Technology Division of Olympus Corporation for the offer of the substrate structure including the multilayer interconnection. The three-dimensional micro-forming processes were performed in the Mechano-Micro Process Laboratory and the Installations for Nano Mechatronics Research in Tokyo Institute of Technology.

7. References

S. Hata, K. Sato and A. Shimokohbe, 1999, "Fabrication of Thin Film Metallic Glass and its Application to Microactuator", Proceedings of SPIE International Symposium on Microelectronics and Micro-Electro-Mechanical Systems MICRO/MEMS'99, 3892, Queensland, Australia, pp. 97-108.

S. Hata, J. Sakurai and A. Shimokohbe, 2005, "Thin Film Metallic Glasses as New MEMS Materials", Technical Digest of The 18th IEEE International Conference on MEMS 2005, Miami, USA, pp. 479-482.

S. Hata, Y. Yamada, J. Ichihara and A. Shimokohbe, 2002, "A Micro Lens Actuator for Optical Flying Head"; Technical Digest of The 15th IEEE International Conference on MEMS 2002, Las Vegas, USA, pp. 507-510.

S. Hata, H. W. Jeong and A. Shimokohbe, 2004, "2-DOF thin film metallic glass microactuator", Proceedings of European Society for Precision Engineering and Nanotechnology (euspen Glasgow 2004), Glasgow, Scotland, pp. 9-10.

A. Inoue, 2000, "Stabilization of metallic supercooled liquid and bulk amorphous alloys", Acta Materialia, Vol.48, Issue 1, 1, pp. 279-306.

Y. Liu, S. Hata, K. Wada and A. Shimokohbe, 2001, "Thermal, Mechanical and Electrical Properties of Pd-based Thin Film Metallic Glass", Jpn. J. Appl. Phys., Vol.40, pp. 5382-5388.

W. N. Sharpe, K. Jackson, K. J. Hemker, and Z. Zie, 2001, "Effect of specimen size on Young's modulus, and strength of polysilicon", J. Microelectromech Syst, vol. 10, pp. 317-326.

T. Fukushige, S. Hata, and A. Shimokohbe, 2005, "A MEMS Conical Spring Actuator Array", IEEE/ASME Journal of Microelectromechanical Systems, Vol. 14, No. 2, pp. 243-253.

Shimokohbe, 2005, "Thin Film Metallic Glass Actuators", http://www.nano.pi.titech.ac.jp/Research/Shimo_Topics/TFMG_Actuator_e.htm.

M.Elwenspoek, L.Smith, and B.Hok, 1992, "Active joints for microrobot limbs", Journal of Micromechanics and Microengineering No.2, pp. 221-223.

Michel A Rosa, Dirk De Bruyker, Armin R Volkel, Eric Peeters and John Dunes, 2004 "A novel external electrode configuration for the electrostatic actuation of MEMS based devices", Journal of Micromechanics and Microengineering No.14, pp. 446-451.

8. Responsibility notice

The authors are the only responsible for the printed material included in this paper.